

Evaluation of partial widths and branching ratios from resonance wave functions

Tamar Goldzak,^{1,2} Ido Gilary,¹ and Nimrod Moiseyev^{1,2,3}

¹*Schulich Faculty of Chemistry, Technion-Israel Institute of Technology, Haifa IL-32000, Israel*

²*Russell-Berrie Nanotechnology Institute, Technion-Israel Institute of Technology, Haifa IL-32000, Israel*

³*Department of Physics, Technion-Israel Institute of Technology, Haifa IL-32000, Israel*

(Received 9 August 2010; published 8 November 2010)

A quantum system in a given resonance state has different open channels for decay. Partial widths are the decay rates of the resonance (metastable) state into the different open channels. Here we present a rigorous derivation of the partial widths from the solution of a time-dependent Schrödinger equation with outgoing boundary conditions. We show that the sum of the partial widths obtained from the resonance wave function is equal to the total width. The difference with respect to previous studies on partial widths and branching ratios is discussed.

DOI: [10.1103/PhysRevA.82.052105](https://doi.org/10.1103/PhysRevA.82.052105)

PACS number(s): 03.65.–w

I. INTRODUCTION

Resonances are metastable states of a system which does not immediately break into its subsystems although it has enough energy to do so. The decay of the system typically takes on an exponential time profile and such states can survive for extremely long or short times depending on the studied system. This phenomenon is very general and plays a key role in many different types of scattering experiments in atomic, molecular, nanostructural, optical, and nuclear physics. See, for example, the pioneering work of Gamow on the subject [1] or Taylor's book on scattering theory [2]. Resonances are obtained in one-particle systems as well as in many-particle systems. Their occurrence is not limited by the dimensionality of the problem. In one-dimensional cases, such as the case of electrons which are temporarily trapped inside a quantum well, the electrons have two open channels for decay. They can either decay to the right lead which is attached to the quantum well or to the left lead. In two-dimensional systems (for example, leaking modes in two-dimensional waveguides [3,4] and the scattering of diatoms from solid surfaces [5]) and three-dimensional systems (e.g., predissociation of a three-atomic molecule [6]) there are several open channels for decay.

The probability of such metastable systems decaying to every one of the open channels varies and determines the ratios between the different decay products which will be obtained. The rate of decay to each of the open channels is also known as the partial width (this nomenclature is evident from the discussion in what follows on the imaginary part of the resonance energy). The ratio between two such rates is known as the branching ratio since it dictates the relative amount of decay products obtained in each of these channels. Knowing the partial widths and branching ratios for a given system in a metastable state is of a vital importance since it may enable one to manipulate the system in order to get a certain product and not another. In this article we show how the partial widths of a system in a resonance state are obtained in a rigorous fashion from the time-dependent Schrödinger equation (TDSE).

Resonance can occur by various mechanisms. Probably the simplest situation which gives rise to such metastable states is in one-dimensional systems where the interaction potential supports a double barrier (see, e.g., Fig.1). In such systems the particle is temporarily trapped between the two barriers

but will eventually decay due to tunneling. Such a quasi-one-dimensional picture is often used to explain resonant tunneling profiles in semiconductor devices. When the threshold energies for the decay of the particle in each direction are different (see Fig. 1), there will be also a difference in the probability to decay to each of the asymptotes.

In more complicated systems involving more degrees of freedom the description of resonances is convenient from the viewpoint of the different decay products or the common terminology of decay channels. In this picture a resonance can be viewed as a bound state of the Hamiltonian in one channel embedded in the continuum of the Hamiltonian of another channel which becomes metastable due to the coupling with the embedding continuum. This state has a finite lifetime and as time passes decays to the reaction products which are defined by the uncoupled open channels. Let us elaborate on this point. Without loss of generality we assume that the system under study consists of two subsystems which interact with one another. The system can be, for example, two interacting particles or one particle which moves in a two-dimensional potential (e.g., quantum wells), a light beam which propagates in two coupled waveguides, etc. The Hamiltonian of the full system is described by

$$H(1,2) = h_1(1) + h_2(2) + V(1,2), \quad (1)$$

where, correspondingly, $h_1(1)$ and $h_2(2)$ are the Hamiltonians for the noninteracting subsystems. The interaction potential $V(1,2)$ vanishes when either one of the two particles is removed from the system (for example, via ionization or dissociation) or when the separation distance between the two quantum-wells or waveguides is sufficiently large. For simplicity, let us assume that the subsystem that can be removed is subsystem "2". The threshold energies are the eigenvalues of the h_2 Hamiltonian,

$$h_2 \chi_n(2) = \epsilon_n^{th} \chi_n(2). \quad (2)$$

The α th eigenfunction of the full Hamiltonian given in Eq. (1) can be expanded in terms of the eigenfunctions of the h_2 Hamiltonian,

$$\Psi_\alpha(1,2) = \sum_{n=1}^N \varphi_{n,\alpha}(1) \chi_n(2), \quad (3)$$

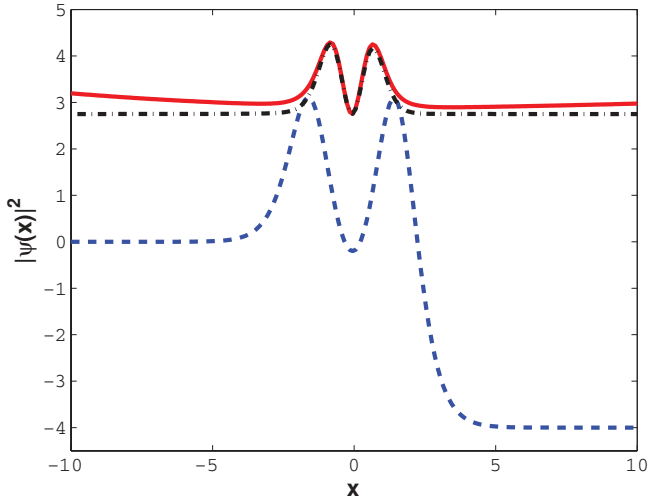


FIG. 1. (Color online) The one-dimensional potential in Eqs. (68) and (69) (dashed line), the scaled function of the second resonance (dash-dotted black line), and the unscaled resonance wave function (solid red line). All values are given in atomic units. The complex resonance energy is composed of the position $\varepsilon_2 = 2.75062$ and width $\Gamma_2 = 0.26519$. Note that while the unscaled resonance function diverges asymptotically, the scaled resonance wave function is square-integrable.

where N is the number of the eigenfunctions of h_2 which serve as a basis set and $\varphi_{n,\alpha}(1)$'s are the n th channel functions labeled by the index α .

As usual, the exact eigenfunction $\Psi_\alpha(1,2)$ of the full Hamiltonian is obtained when $N \rightarrow \infty$ in the variational calculations where a set of coupled secular equations are solved and are represented as an eigenvalue matrix problem,

$$\mathbf{H}\boldsymbol{\varphi}_\alpha(1) = E_\alpha\boldsymbol{\varphi}_\alpha(1), \quad (4)$$

where $\boldsymbol{\varphi}_\alpha$ are vectors containing the channel function $\varphi_{n,\alpha}(x)$. The operators on the diagonal of the Hamiltonian matrix \mathbf{H} are given by

$$H_{n,n} = h_1(1) + \mathcal{V}_n^{\text{eff}}(1), \quad (5)$$

where

$$\mathcal{V}_n^{\text{eff}}(1) = \langle \chi_n(2) | V(1,2) | \chi_n(2) \rangle_2 + \epsilon_n^{\text{th}}. \quad (6)$$

Here the notation $\langle \cdot \rangle_2$ represents integration over all space on the coordinates of subsystem 2. The bound states of the n th closed channel for decay are associated with the eigenvalues of $H_{n,n}$ which are below the threshold energies ϵ_n^{th} . There are bound states of the n th channel which are embedded in the continuum of the $H_{n',n'}$ effective Hamiltonian where $n' < n$. The n' effective Hamiltonians are the open channels for decay. This is due to the introduction of the coupling potential terms $H_{n,n'} = \int \varphi_n^*(2) V(1,2) \varphi_{n'}(2) d\tau_2$ between the closed and open channels. Consequently, the bound states of the $H_{n,n}$ effective Hamiltonians become metastable when coupled to the continuum of the open channels. The calculations of the so-called resonance states, are briefly described in what follows.

A. The resonance energy and wave function

The resonances are associated with the poles of the scattering matrix where there is only a flux of outgoing particles [2]. Therefore, they are associated with the solutions of the Schrödinger equation which are obtained under the requirement of outgoing boundary conditions (see, e.g., Ref. [7]). In the case of multichannel problems, the outgoing boundary conditions are imposed on the eigenfunctions of the Hamiltonian given in Eq. (4). That is, the asymptotes of every one of the components of the eigenfunctions $\varphi_{n,\alpha}$ are given by

$$\varphi_{n,\alpha}(1) \rightarrow A_{n,\alpha} e^{ik_{n,\alpha}r_1}, \quad (7)$$

where

$$k_{n,\alpha} = \frac{\sqrt{2m(E_\alpha - \epsilon_n^{\text{th}})}}{\hbar} \quad (8)$$

and m is the mass of the free particle. For the closed channels for decay which are denoted by n_c , the wave vectors $k_{n,\alpha}$ are purely imaginary numbers and therefore

$$\varphi_{n_c,\alpha}(1) \rightarrow A_{n_c,\alpha} e^{-|k_{n_c,\alpha}|r_1}. \quad (9)$$

For the open channels for decay which are denoted by n_o , the wave vector $k_{n,\alpha}$ gets complex values (with negative-value imaginary parts) and therefore the asymptotes of the open channels exponentially diverge:

$$\varphi_{n_o,\alpha}(1) \rightarrow A_{n_o,\alpha} e^{i\text{Re}[k_{n_o,\alpha}]r_1} e^{+\text{Im}[k_{n_o,\alpha}]r_1} \rightarrow \infty. \quad (10)$$

The resonance energies E_α are complex where the total rate of decay is defined by the imaginary part of the complex energy:

$$\Gamma_\alpha = -2\text{Im}[E_\alpha]. \quad (11)$$

The resonance energies can be obtained by various techniques and procedures developed over the years. These include, to name a few, the variety of complex coordinate methods [8], Siegert pseudostates [9] and Feshbach projection operator techniques [10].

B. Open question regarding partial widths

Partial widths are important physical properties whenever we are interested in the relative probability of obtaining any of the decay products of a given metastable system. They also play a part in explaining resonant transmission profiles. Since the partial widths of the resonance represent a measurable physical quantity which determines the amount of each of the various decay products, we should be able to attain them in a rigorous fashion from the solution to the Schrödinger equation.

Partial widths are extracted in the literature by various methods. In many cases, due to certain approximations in the calculation, the sum of the partial widths does not add up to the total width of the resonance. See, for example, Refs. [11] and [12]. As previously pointed out [13,14], it is possible to calculate the partial widths from the analysis of the tail of the square-integrable complex scaled wave functions. This method has been used in Ref. [15] to calculate the partial widths for Noro-Taylor model Hamiltonian [16] motivated by the idea

of using this approach for calculating the partial widths in nuclear scattering experiments. Numerical calculations have shown that the sum over all the partial widths calculated by the analysis of the tail of the resonance wave function is about equal to the resonance width Γ_α . However, it is not clear if the deviation of $\sum_{n_o} \Gamma_{n_o,\alpha} / \Gamma_\alpha$ from unity results from numerical errors in obtaining the information from the tail of the complex scaled resonance function which exponentially decays to zero.

In previous studies, García-Calderón *et al.* [17,18] obtained the partial widths for finite-range potentials in a manner which ensures that the partial widths will add up exactly to the total width. This was achieved by evaluating the outgoing flux from the relevant region of interaction at the boundaries where the potential vanishes.

The open question we address in this article is how to evaluate the partial widths from the tail of the resonance wave function in a manner which will be independent of the potential parameters and will ensure that

$$\sum_{n_o} \Gamma_{n_o,\alpha} = \Gamma_\alpha. \quad (12)$$

We show here that by analyzing the time dependence of the resonance wave function itself, we are not restricted to an exact definition of an interaction region and can apply our formalism to smooth potentials regardless of their parameters. For simplicity, in Sec. II we start with a general one-dimensional formulation for a single particle. We then move on to the more complicated but rather similar formulation of multidimensional problems in Sec. III. In Sec. IV we illustrate our findings with some numerical examples. We then proceed to discuss in Sec. V the conditions which will emphasize our results before concluding in Sec. VI.

II. PARTIAL WIDTHS IN ONE-DIMENSIONAL POTENTIALS

In one dimension a particle trapped in a resonance state can decay only to two different “channels”—the asymptotes at $\pm\infty$. Accordingly, we refer to the partial width in each of these directions as Γ_\pm , respectively. The starting point for the derivation will be the one-dimensional continuity equation which results directly from the TDSE:

$$\frac{\partial}{\partial t} \rho(x,t) + \frac{\partial}{\partial x} j(x,t) = 0, \quad (13)$$

where the time-dependent probability density $\rho(x,t)$ is

$$\rho(x,t) = |\psi(x,t)|^2 \quad (14)$$

and the probability current $j(x,t)$ is given by

$$j(x,t) = \frac{\hbar}{m} \text{Im} \left[\psi^*(x,t) \frac{\partial}{\partial x} \psi(x,t) \right]. \quad (15)$$

We now want to study the implications of Eq. (13) for a single resonance state of the problem. This means we impose outgoing boundary conditions on the solution of the time-independent Schrödinger equation (TISE):

$$\hat{H}\phi(x) = E_{\text{res}}\phi(x). \quad (16)$$

In other words, we are looking for solutions which satisfy

$$[\hat{p}_x \pm \hbar k_\pm] \phi(x \rightarrow \pm\infty) = 0, \quad (17)$$

where $\pm\hbar k_\pm$ is the momentum of the outgoing particles in each direction given by

$$k_\pm = \frac{\sqrt{2m(E_{\text{res}} - E_\pm^{\text{th}})}}{\hbar} = k_\pm^{\text{Re}} - ik_\pm^{\text{Im}}. \quad (18)$$

Here the threshold for escape in each direction is E_\pm^{th} and the resonance energy E_{res} is complex due to the restricting boundary conditions such that

$$E_{\text{res}} = \varepsilon - i \frac{\Gamma}{2}. \quad (19)$$

In the asymptotes these solutions will behave as

$$\phi(x \rightarrow \pm\infty) = A_\pm e^{\pm ik_\pm x} = A_\pm e^{\pm ik_\pm^{\text{Re}} x} e^{k_\pm^{\text{Im}} |x|}. \quad (20)$$

A resonance solution to the TDSE is given accordingly by

$$\psi(x,t) = e^{-iE_{\text{res}}t/\hbar} \phi(x,t). \quad (21)$$

This means that the probability density decays uniformly exponentially in time,

$$\rho(x,t) = e^{-\Gamma t/\hbar} \rho(x,0), \quad (22)$$

and the derivative in time of this probability density is simply

$$\frac{\partial \rho(x,t)}{\partial t} = -\frac{\Gamma}{\hbar} \rho(x,0). \quad (23)$$

The flux at any given point will also decay exponentially in time but due to the spatially diverging properties of the resonance state it will also diverge exponentially in the asymptotes. These two seemingly contradicting trends are addressed shortly in what follows. The flux at the asymptotes is accordingly given by

$$j(x \rightarrow \pm\infty, t) = \frac{\pm\hbar k_\pm^{\text{Re}}}{m} |A_\pm|^2 e^{2k_\pm^{\text{Im}} |x|} e^{-\Gamma t/\hbar}. \quad (24)$$

Since in Eqs. (23) and (24) the only time dependence is in the exponent, we can eliminate the time dependence from the continuity equation in Eq. (13) after taking the derivative in time of the probability density. By integrating Eq. (13) over a finite range, $[-L_-, L_+]$, we can relate between the flux at the boundaries $j(\pm L_\pm)$ and the decay of the total probability density inside this region,

$$-[j(L_+) - j(-L_-)] = -\frac{\Gamma}{\hbar} N_L, \quad (25)$$

where N_L is the initial probability inside the region $[-L_-, L_+]$,

$$N_L = \int_{-L_-}^{L_+} |\phi(x)|^2 dx. \quad (26)$$

We have two competing processes (decay to the left and to the right). The rate of each process depends on the total probability N_L such that the two rates add up to the total rate: $\Gamma_+ + \Gamma_- = \Gamma$. Thus, the contribution to the total width through the flux in each direction is defined by

$$\Gamma_\pm = \pm \frac{\hbar j(\pm L_\pm)}{N_L} = \frac{\hbar^2 k_\pm^{\text{Re}}}{m N_L} |A_\pm|^2 e^{2k_\pm^{\text{Im}} L_\pm}. \quad (27)$$

Equation (27) is parallel to Eqs. (8) and (9) of Ref. [18]. It is evident that although in Eq. (27) we have ensured that $\Gamma_+ + \Gamma_- = \Gamma$, this definition of the partial widths still depends on where we choose to measure the flux. This is in a sense analogous physically to putting detectors at L_\pm . Since the asymptotic divergence in each of the channels which depends on k_\pm^{Im} is inherently nonphysical, changing the boundary can lead to very different and even contradicting results. This leads naturally to the question of where the correct place to measure the flux would be. In finite-range potentials the natural choice will be the point where the potential vanishes. Generally, we need to define our interaction region in a way which adheres to the physical nature of the decay of the resonance. This problem will also manifest itself in the branching ratio between the two possible decay products given by

$$R = \frac{\Gamma_+}{\Gamma_-} = \frac{k_+^{\text{Re}} |A_+|^2}{k_-^{\text{Re}} |A_-|^2} e^{2(k_+^{\text{Im}} L_+ - k_-^{\text{Im}} L_-)}. \quad (28)$$

Consider, for instance, the situation where we place the boundaries L_\pm at the same distance from the origin and find, for instance, that there is a strong preference to decay to $-\infty$. If we now move only the right boundary due to the spatial divergence of the wave function, we will get that Γ_+ will diverge. This will also cause N_L to diverge, and thus Γ_- will vanish and we will get a complete opposite trend.

How can this discrepancy be settled? We can reach a resolution if we understand the ‘‘physical nature’’ of the resonance wave function. When we try to describe a resonance state over the whole range of space and time, we have a problem. This is because a resonance is constantly decaying; therefore, it had to decay also infinitely long ago. In addition, the probability has to go somewhere, but if we consider the whole space it has nowhere to decay to. This is the source for the large accumulation of probability at the asymptotes, which is in a sense compensated by the temporal decay of the wave function. In order to describe a more realistic situation, we have to consider some initial time when the decay is initiated, as well as some restricted part of space where the probability can decay from. Using this reasoning in Ref. [19], Hatano *et al.* considered a more physical situation of a resonance which starts emanating at some time $t = 0$ from a finite region which expands at the speed of the escaping particles. Using this description of a resonance state, the authors showed that the total probability inside the confining region in this state is conserved.

We use similar reasoning here. The main difference is that here the escaping particles possess different velocities in each direction. Thus, we have to allow the volume to expand at a different rate in every direction. Accordingly, we define our volume of interest using time-dependent boundaries given by

$$L_\pm = \frac{\hbar k_\pm^{\text{Re}}}{m} t. \quad (29)$$

Note that by considering such a moving boundary we settled the ‘‘competition’’ between the exponential decay in time and the exponential divergence in space which we observed in the

flux in Eq. (24) and when we look at the flux on the boundaries of the confined region we get

$$j(L_\pm(t)) = \frac{\pm \hbar k_\pm^{\text{Re}}}{m} |A_\pm|^2 e^{2k_\pm^{\text{Im}} L_\pm - \Gamma t / \hbar}. \quad (30)$$

In the exponent in Eq. (30) we have now

$$2k_\pm^{\text{Im}} \frac{\hbar k_\pm^{\text{Re}}}{m} t - \frac{\Gamma}{\hbar} t = 0. \quad (31)$$

This term vanishes since the width of the resonance is a product of the real and the imaginary parts of the wave vector in each direction,

$$\Gamma = \frac{2\hbar^2 k_\pm^{\text{Re}} k_\pm^{\text{Im}}}{m}. \quad (32)$$

Thus, we see that on the moving boundary we have a constant flux. Substituting the moving boundaries in the integration over the flux equation (after taking the time derivative of the probability density) and subsequently in Eqs. (27) and (28) yields a well-defined branching ratio. In the exponent in Eq. (28) we have now

$$k_+^{\text{Im}} \frac{\hbar k_+^{\text{Re}}}{m} t - k_-^{\text{Im}} \frac{\hbar k_-^{\text{Re}}}{m} t. \quad (33)$$

This term vanishes again due to Eq. (32). So we have established that the branching ratio is given by

$$R = \frac{\Gamma_+}{\Gamma_-} = \frac{k_+^{\text{Re}} |A_+|^2}{k_-^{\text{Re}} |A_-|^2}, \quad (34)$$

while the partial widths are given by

$$\Gamma_\pm = \frac{\hbar^2 k_\pm^{\text{Re}} |A_\pm|^2}{m} \left[\frac{e^{+\Gamma t / \hbar}}{N_L(t)} \right]. \quad (35)$$

$N_L(t)$ is the probability density of the initial resonance wave function inside the expanding region $[-L_-, L_+]$, which is given by

$$N_L(t) = \int_{-L_-(t)}^{L_+(t)} |\phi(x)|^2 dx. \quad (36)$$

It may seem as if these partial widths are time dependent, but the increase of $N_L(t)$ is proportional to the increase in the flux in each channel due to the divergence of $\phi(x)$ at the asymptotes and therefore the partial widths are constant. That is,

$$\lim_{t \rightarrow \infty} \left[\frac{e^{+\Gamma t / \hbar}}{N_L(t)} \right] = \text{const.} \quad (37)$$

This is clearly evident if we express them through the branching ratio and the total width:

$$\Gamma_+ = \frac{\Gamma}{1 + R^{-1}}; \quad \Gamma_- = \frac{\Gamma}{1 + R}. \quad (38)$$

Therefore, all the information we need is the behavior of the resonance wave function at each of the asymptotes; that is, we need to know k_\pm and A_\pm .

III. PARTIAL WIDTHS IN MULTICHANNEL PROBLEMS

We now consider a system which has many degrees of freedom which we label $\{x_1, x_2, \dots, x_N\}$. Assuming that we wish to examine several of these coordinates (for instance,

these could be the coordinates along which dissociation can occur), we label them $\mathbf{x} = \{x_1, x_2, \dots, x_M\}$, while the remaining coordinates are labeled $\mathbf{y} = \{x_{M+1}, \dots, x_N\}$. In general, we can write the Hamiltonian in these coordinates in a similar manner to Eq. (1) as

$$\hat{H} = \hat{h}_x(\mathbf{x}) + \hat{h}_y(\mathbf{y}) + V(\mathbf{x}, \mathbf{y}). \quad (39)$$

Choosing an orthonormal basis in the \mathbf{y} coordinates $\{\chi_n(\mathbf{y})\}$, we can write the general solution of the Schrödinger equation as

$$\psi(\mathbf{x}, \mathbf{y}, t) = \sum_n \varphi_n(\mathbf{x}, t) \chi_n(\mathbf{y}). \quad (40)$$

A convenient choice for $\{\chi_n(\mathbf{y})\}$ which sets the ground for intuitive physical interpretation of the system is simply to take the eigenstates of \hat{h}_y . This leads to a set of coupled equations,

$$\begin{pmatrix} \hat{h}_x + V_{11} & V_{12} & \cdots \\ V_{21} & \hat{h}_x + V_{22} & \cdots \\ \vdots & \vdots & \ddots \end{pmatrix} \begin{pmatrix} \varphi_1 \\ \varphi_2 \\ \vdots \end{pmatrix} = i\hbar \frac{\partial}{\partial t} \begin{pmatrix} \varphi_1 \\ \varphi_2 \\ \vdots \end{pmatrix}, \quad (41)$$

which is just the matrix form of the TDSE: $\mathbf{H}\boldsymbol{\varphi} = i\hbar \frac{\partial}{\partial t} \boldsymbol{\varphi}$, where

$$H_{m,n} = \hat{h}_x(\mathbf{x})\delta_{m,n} + V_{m,n}(\mathbf{x}), \quad (42)$$

$$V_{m,n}(\mathbf{x}) = \langle \chi_m(\mathbf{y}) | \hat{h}_y(\mathbf{y}) + V(\mathbf{x}, \mathbf{y}) | \chi_n(\mathbf{y}) \rangle_y.$$

Here the notation $\langle \cdot \rangle_y$ implies integration over the \mathbf{y} coordinates only. The diagonal terms of $H_{n,n}$ define the channels of the problem which are coupled to each other through the off-diagonal terms $V_{n,m}$. In order to arrive at an equation relating the flux at each channel with the probability density, we have to integrate the N -dimensional continuity equation over all the \mathbf{y} coordinates,

$$\frac{\partial}{\partial t} \rho(\mathbf{x}, \mathbf{y}, t) + \nabla \cdot \mathbf{j}(\mathbf{x}, \mathbf{y}, t) = 0, \quad (43)$$

where $\rho(\mathbf{x}, \mathbf{y}, t) = |\psi(\mathbf{x}, \mathbf{y}, t)|^2$ is the probability density and $\mathbf{j}(\mathbf{x}, \mathbf{y}, t)$ is the probability flux. When the potential is real, this integration leads to the following result:

$$\frac{\partial}{\partial t} \sum_n \rho_n(\mathbf{x}, t) + \nabla_x \cdot \sum_n \mathbf{j}_n(\mathbf{x}, t) = 0, \quad (44)$$

where the probability density in each channel is given by

$$\rho_n(\mathbf{x}, t) = |\varphi_n(\mathbf{x}, t)|^2 = |\langle \chi_n(\mathbf{y}) | \psi(\mathbf{x}, \mathbf{y}, t) \rangle_y|^2. \quad (45)$$

For a single particle the current density in each of the channels is

$$\mathbf{j}_n(\mathbf{x}, t) = \frac{\hbar}{m} \text{Im}[\varphi_n^*(\mathbf{x}, t) \nabla_x \varphi_n(\mathbf{x}, t)]. \quad (46)$$

In order to obtain the partial widths for this general case, we need to integrate Eq. (44) over a finite volume in space. Here we can make use of the divergence theorem which will allow us to convert the volume integral over the current to the outgoing flux on the surface bounding the chosen volume. For simplicity, we consider now just one dissociative coordinate x in the range of $x \in [0, \infty]$, where dissociation can occur only when

$x \rightarrow \infty$. To obtain partial widths and branching ratios, we substitute a resonance solution. The resonance wave function reads

$$\psi(x, \mathbf{y}, t) = e^{-iE_{\text{res}}t/\hbar} \psi(x, \mathbf{y}, 0). \quad (47)$$

Using the expansion Eq. (40), we get the wave function in each channel by

$$\varphi_n(x, t) = e^{-iE_{\text{res}}t/\hbar} \langle \chi_n(\mathbf{y}) | \psi(x, \mathbf{y}, 0) \rangle_y. \quad (48)$$

Accordingly, the asymptotic behavior in each of the channels is given by

$$\varphi_n(x \rightarrow \infty, t) = A_n e^{-iE_{\text{res}}t/\hbar} e^{ik_n x}, \quad (49)$$

where the outgoing wave vector in each of the channels is determined by the respective threshold energy, E_n^{th} ,

$$k_n = \frac{\sqrt{2m(E_{\text{res}} - E_n^{\text{th}})}}{\hbar} = k_n^{\text{Re}} - ik_n^{\text{Im}}. \quad (50)$$

Consequently, the probability density in each channel in Eq. (45) when we have a resonance state is given by

$$\rho_n(x, t) = e^{-\Gamma t/\hbar} |\langle \chi_n(\mathbf{y}) | \psi(\mathbf{x}, \mathbf{y}, 0) \rangle_y|^2, \quad (51)$$

and the flux in each channel in Eq. (46) for a resonance state is

$$j_n(x, t) = e^{-\Gamma t/\hbar} \frac{\hbar}{m} \text{Im}[\varphi_n^*(x, 0) \nabla_x \varphi_n(x, 0)]. \quad (52)$$

The uniform time dependence enables us in a similar fashion to the one-dimensional case to take the time derivative in Eq. (44) and eliminate time from the continuity equation:

$$\frac{\partial}{\partial x} \sum_n j_n(x) = \frac{\Gamma}{\hbar} \sum_n \rho_n(x). \quad (53)$$

The current density in the asymptotes of each of the channels is now given by

$$j_n(x \rightarrow \infty) = \frac{\hbar k_n^{\text{Re}}}{m} |A_n|^2 e^{2k_n^{\text{Im}} x}. \quad (54)$$

When we now come to integrate Eq. (53) over a finite region in the x coordinate, we have only one available boundary which leads to

$$\sum_n j_n(L) = \frac{\Gamma}{\hbar} \sum_n N_n, \quad (55)$$

where

$$N_n^L = \int_0^L \rho_n(x, 0) dx. \quad (56)$$

However, as we have seen in Sec. II, in order to obtain a consistent result, we must allow for different boundaries in each of the channels. It is imperative to show that in Eq. (55) we can extend the integration to different values of L for the different channels. That is, we want to check if the following equality also holds:

$$\sum_n j_n(L_n) = \frac{\Gamma}{\hbar} \sum_n N_n. \quad (57)$$

To this end, let us assume that we integrated Eq. (44) up to some minimal value of $L = L_{\text{min}}$, which is in the asymptotic

region of all the channels. This means that on the left-hand side of Eq. (57) we added

$$\sum_n j_n(L_n) - j_n(L_{\min}) = \sum_n \frac{\hbar k_n^{\text{Re}}}{m} |A_n|^2 e^{2k_n^{\text{Im}}(L_n - L_{\min})}, \quad (58)$$

whereas on the right-hand side of Eq. (57) we added

$$\frac{\Gamma}{\hbar} \sum_n \int_{L_{\min}}^{L_n} \rho_n(x, 0) dx = \sum_n \frac{\Gamma |A_n|^2}{2\hbar k_n^{\text{Im}}} e^{2k_n^{\text{Im}}(L_n - L_{\min})}. \quad (59)$$

Using the fact that

$$\Gamma = \frac{2\hbar^2 k_n^{\text{Re}} k_n^{\text{Im}}}{m}, \quad (60)$$

we see that what we added on both sides is identical and thus the equality in Eq. (57) holds when $L = L_{\min}$. This result should be obvious once we realize that in the asymptotes the channels are uncoupled and thus we can add to each channel whatever we want as long as we maintain the continuity of probability in that channel.

It is now possible to use the same reasoning of Sec. II and allow the boundary in each of the channels to expand according to the velocity of the escaping particles in that channel:

$$L_n(t) = \frac{\hbar k_n^{\text{Re}}}{m} t. \quad (61)$$

Now if we define the partial width as

$$\Gamma_n = \frac{\hbar^2 k_n^{\text{Re}}}{m \sum_n N_n^{\text{Im}}(t)} |A_n|^2 e^{2k_n^{\text{Im}} L_n(t)}, \quad (62)$$

where

$$N_n^{\text{Im}}(t) = \int_0^{L_n(t)} \rho_n(x, 0) dx, \quad (63)$$

we get that, due to Eq. (60), the branching ratios are well defined and given by

$$R_{n,n'} = \frac{\Gamma_n}{\Gamma_{n'}} = \frac{k_n^{\text{Re}} |A_n|^2}{k_{n'}^{\text{Re}} |A_{n'}|^2}. \quad (64)$$

This definition ensures us, due to Eq. (57), that the sum over all the partial widths will add up to the total width; that is, $\Gamma = \sum_n \Gamma_n$. This also means that knowing all the branching ratios we can evaluate the partial width in a more convenient manner through the branching ratios:

$$\Gamma_n = \frac{\Gamma}{1 + \sum_{n' \neq n} R_{n',n}} = \frac{|A_n|^2 k_n^{\text{Re}}}{\sum_{n'} |A_{n'}|^2 k_{n'}^{\text{Re}}}. \quad (65)$$

It is evident that all the information we need can be extracted from the asymptote of the wave function and the resonance energy. Therefore, even though our analysis was based on the Hermitian TDSE, we can extract all the necessary information from a non-Hermitian time-independent calculation.

IV. ILLUSTRATIVE NUMERICAL EXAMPLES

To illustrate the finding of the previous sections regarding the branching ratios and partial widths, we need to calculate the amplitude of the resonance wave function in the asymptotes. We find the resonances by a complex scaling technique where

the dissociative coordinate x is scaled by a complex factor such that $x \rightarrow x e^{i\theta}$. This is one of a class of similarity transformations \hat{S}_θ (see the review in Ref. [8]) which render the originally exponentially diverging resonance wave functions square integrable. In other words, via the complex scaling procedure the obtained resonance wave functions are embedded in the generalized Hilbert space such that for one-dimensional systems,

$$\hat{S}_\theta \phi(x) \rightarrow 0, \quad (66)$$

while in multichannel problems in every channel we get

$$\hat{S}_\theta \varphi_n(x) \rightarrow 0 \quad (67)$$

as $x \rightarrow \infty$. The diagonalization of the complex-scaled Hamiltonian matrix yields eigenvalues which give the resonance energies in Eq. (19). The eigenvectors give the scaled form $\phi(x e^{i\theta})$ of the resonance wave functions in Eq. (16). These behave in the asymptotes according to Eq. (20), with the momentum $\pm \hbar k_\pm$ in each of the different open channels. Another method we used to evaluate the resonance wave functions was to solve the Schrödinger equation numerically using a Runge-Kutta method with the requirement of the outgoing boundary condition at the resonance energies we found by complex scaling.

A. Single particle one-dimensional model Hamiltonian

The first example we show here is a one-dimensional nonsymmetric potential, that is, a double barrier with two different threshold energies. The potential is given by

$$V(x) = V_1(x) + V_2(x) - c, \quad (68)$$

where each one of the potentials $V_{1,2}(x)$ is given by

$$V_{1,2}(x) = \frac{a_{1,2}}{\cosh^2(x - b_{1,2})} - \tanh(x - b_{1,2}). \quad (69)$$

In the calculation we used the parameters $a_1 = 6$, $b_1 = 1.5$, $a_2 = 4$, $b_2 = -1.5$, and $c = 2$. The resonance in this potential is a shape resonance and its partial widths reflect the rate of tunneling through the potential barriers on each side. Figure 1 shows that the resonance wave function is localized in the interaction area, and in the asymptotes it diverges in the unscaled form and converges in the scaled form. To calculate the amplitudes A_\pm from the complex scaled wave function ϕ_θ , we need to scale Eq. (20) by $e^{i\theta}$ such that

$$\phi_\theta(x \rightarrow \pm\infty) = A_\pm e^{\pm i k_\pm x e^{i\theta}}, \quad (70)$$

thus yielding

$$A_\pm = \frac{\phi_\theta(x \rightarrow \pm\infty)}{e^{\pm i k_{\text{res}}^\pm x e^{i\theta}}}. \quad (71)$$

The scaled resonance wave function is normalized according to the biorthogonal c product [20], which means that $\int \phi^2(x) dx = 1$. Figure 2 shows how the value of the resonance wave function amplitude $|A_\pm|^2$ stabilizes beyond the interaction area but diverges at the far asymptotes due to numerical errors.

Previous studies on evaluating branching ratios and partial widths from the resonance wave function mostly rely on the

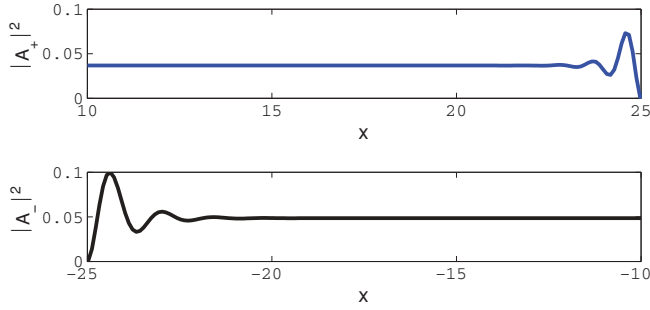


FIG. 2. (Color online) The asymptotic amplitude in both channels of the resonance wave function shown in Fig. 1 given in atomic units.

formula derived by Moiseyev-Peskin (MP) (see Ref. [13]), which gives the branching ratio between any two channels α and β as

$$R_{\alpha,\beta}^{\text{MP}} = \frac{|k_\beta A_\beta^2|}{|k_\alpha A_\alpha^2|}, \quad (72)$$

such that the partial widths are given by

$$\Gamma_{\alpha,\beta}^{\text{MP}} = \frac{\hbar^2}{m} |k_{\alpha,\beta} A_{\alpha,\beta}^2|. \quad (73)$$

Note that in this case we obtain the partial widths from the normalized complex scaled resonance wave function, and thus we do not enforce that $\Gamma_+ + \Gamma_- = \Gamma$. We wish to see how extracting the partial widths and branching ratios from the complex scaled wave function in this method differs from what we proposed here in Sec. II, which, as we have shown, is rigorous. To illustrate this, we calculated the MP branching ratios and partial widths by the MP method and compared them with the new formulas for branching ratios and partial widths, which we label GGM. These were given in Eqs. (34) and (35). Table I gives a comparison between the two methods for a few resonances of the model one-dimensional Hamiltonian we chose. From Table I one can conclude that the old formula gives good results and the sum of the partial width is almost equal to the total width for narrow resonances. For broad resonances evaluating the partial width from the normalized complex scaled resonance wave function does not yield a good result as the partial widths do not add up to the total width. It is interesting to note that for the branching ratios the difference between the two methods is not significant even for broad resonances. Thus, if we renormalize the resonance wave function such that $\Gamma_+ + \Gamma_- = \Gamma$, the results of the two methods will be very similar for all resonances in this model. This point is addressed in Sec. V

B. Single-particle 3D model Hamiltonian

The second example we give here is the Noro-Taylor model Hamiltonian [16], which was used before in similar studies on branching ratios and partial widths. This is a model of two coupled channels for spherical s -waves where the Hamiltonian potential matrix elements are given by

$$V_{i,j}(x) = \lambda_{i,j} x^2 e^{-x} + E_j^{\text{th}} \delta_{i,j}. \quad (74)$$

TABLE I. Values of the partial widths and branching ratios obtained by the method in Ref. [13] (MP) and the method presented in this article (GGM) in Eqs. (35) and (34) for the model 1D potential in Fig. 1 (all values in atomic units).

	E_{res}	Method	Γ_-	Γ_+	$\Gamma_- + \Gamma_+$	$R = \frac{\Gamma_+}{\Gamma_-}$
ε_1	0.877 06	MP	0.000 83	0.004 14	0.004 97	4.796 03
Γ_1	0.004 98	GGM	0.004 12	0.000 86	0.004 98	4.796 38
ε_2	2.750 62	MP	0.135 09	0.113 90	0.248 99	1.112 53
Γ_2	0.265 19	GGM	0.125 52	0.139 67	0.265 19	1.112 80
ε_4	5.501 30	MP	1.087 37	1.410 34	2.497 71	1.242 40
Γ_4	4.881 51	GGM	2.159 94	2.721 57	4.881 51	1.260 02

This is in the range $x \in [0, \infty]$, where the $\lambda_{i,j}$ parameters are given by the following matrix λ :

$$\lambda = \begin{pmatrix} -1 & -7.5 \\ -7.5 & 7.5 \end{pmatrix}. \quad (75)$$

The threshold energies are $E_1^{\text{th}} = 0$ and $E_2^{\text{th}} = 0.1$. This coupled channel problem where in each of the channels we have an effective one-dimensional Hamiltonian has resonances which possess both Feshbach-type character due to the coupling between the bound state in the closed channel and the continuum of the open channel as well as shape-type character due to the tunneling through the barrier in the open channel.

Figure 3 presents a resonance function in the two channels. Like we observed for the 1D potential also, here the resonance wave function is localized in the interaction area, and in the asymptotes it is diverging for the unscaled function and converging for the scaled function. The amplitude of the function in the asymptotes is calculated in the same manner as the one-dimensional case in Eq. (71). In Table II we compare the MP method from Refs. [13,21] and Eqs. (73) and (72) with our derivation (GGM) from Eqs. (62) and (64), respectively.

We can see in Table II that for the first resonance in the NT model, which is a very narrow resonance, the partial widths sum up to the total width in the old formula and there is no change at all in the branching ratio between the old and the new formulas. In the broad resonances one can see that the broader the resonance, the less accurate is Eq. (73), but the branching ratio formula does not see a significant change. This result is

TABLE II. Values of partial widths and branching ratios calculated by the MP method in Eqs. (73) and (72) and by the method derived in Eqs. (62) and (64) in Sec. III for the Noro-Taylor model (all values in atomic units).

	E_{res}	Method	Γ_1	Γ_2	$\Gamma_1 + \Gamma_2$	$R = \frac{\Gamma_2}{\Gamma_1}$
ε_1	4.768 20	MP	0.000 05	0.001 37	0.001 42	0.037 72
Γ_1	0.001 42	GGM	0.000 05	0.000 86	0.001 42	0.037 72
ε_2	7.241 20	MP	0.523 75	1.677 10	2.200 85	0.316 37
Γ_2	1.511 91	GGM	0.363 51	1.148 40	1.511 91	0.316 54
ε_4	8.440 53	MP	12.054 83	35.476 20	47.531 03	0.339 80
Γ_4	12.562 99	GGM	3.188 49	9.374 49	12.562 99	0.340 12

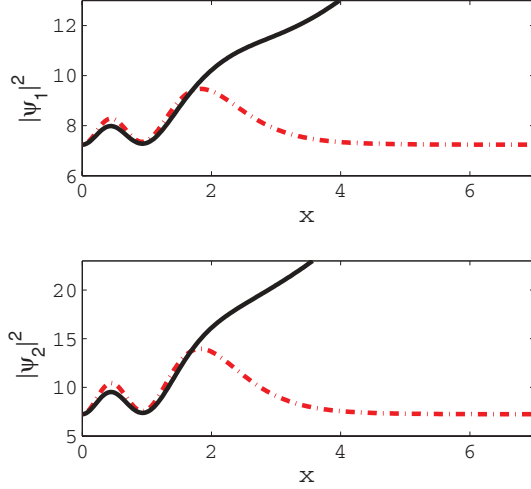


FIG. 3. (Color online) The Noro-Taylor resonance wave function with position $\varepsilon_2 = 7.24120$ and width $\Gamma = 1.51191$. The scaled (dashed red line) and unscaled (solid black line) functions are shown in each of the channels. All values are given in atomic units. Note that the unscaled resonance function diverges asymptotically while the scaled resonance wave function is square integrable.

important in view of the use of the MP formalism for the evaluation of branching ratios in nuclear physics problems [15].

V. DISCUSSION

As we see in the previous section in the two examples we studied there is no significant difference between the old formulas commonly used for evaluating branching ratio in Eq. (72) [13,14] and the formula we propose following our derivation here in Eq. (64). This is in fact a very general result and in most cases there would not be a significant difference between using the “old” and the “new” formulas. In order to understand this general result, let us take a closer look into the two expressions.

The old formula for the branching ratio between two channels is given in Eq. (72):

$$R_{\text{old}} = \left| \frac{k_2 A_2^2}{k_1 A_1^2} \right|. \quad (76)$$

The new formula for the branching ratio is given in Eq. (64):

$$R_{\text{new}} = \frac{k_2^{\text{Re}} |A_2|^2}{k_1^{\text{Re}} |A_1|^2}. \quad (77)$$

We see that the only difference is in using the real or the absolute part of $k_{1,2}$. Therefore, we now try to find a more “telling” relation between these values:

$$\gamma = \left| \frac{k_2}{k_1} \right| = \sqrt{\frac{(k_2^{\text{Re}})^2 + (k_2^{\text{Im}})^2}{(k_1^{\text{Re}})^2 + (k_1^{\text{Im}})^2}} = \frac{k_2^{\text{Re}}}{k_1^{\text{Re}}} \sqrt{\frac{1 + z_2^2}{1 + z_1^2}}, \quad (78)$$

where

$$z_{1,2} = \frac{k_{1,2}^{\text{Im}}}{k_{1,2}^{\text{Re}}}. \quad (79)$$

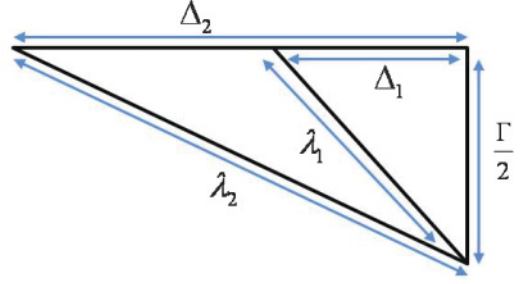


FIG. 4. (Color online) A geometrical representation of the distance of the resonance from the two thresholds $E_{1,2}^{\text{th}}$. $\Delta_{1,2}$ are the distances of the resonance position ε from the two thresholds $E_{1,2}^{\text{th}}$, respectively, while $\lambda_{1,2}$ are the distances of the resonance from the two thresholds $E_{1,2}^{\text{th}}$, respectively.

First we see that for narrow isolated resonances it is clear that, since the imaginary part of $k_{1,2}$ is small, $z_{1,2}$ is very small and has small contribution to the branching ratio. Second, we must realize that the expression in Eq. (78) already puts strong restrictions on the differences we might observe between the two methods. Since the wave vector in each of the channels must lie in the fourth quadrant of the corresponding k plane over the 45° bisector, we know that $0 \leq z_{1,2} \leq 1$; thus, we know that γ falls in the range of

$$\frac{\sqrt{2} k_2^{\text{Re}}}{2 k_1^{\text{Re}}} \leq \gamma \leq \sqrt{2} \frac{k_2^{\text{Re}}}{k_1^{\text{Re}}}. \quad (80)$$

To get a more general intuition into what conditions must be satisfied in order to see a significant effect, we must remember that the momenta are related to the complex energy through

$$\frac{\hbar^2}{m} k_{1,2}^{\text{Re}} k_{1,2}^{\text{Im}} = \frac{\Gamma}{2}, \quad (81)$$

$$\frac{\hbar^2}{2m} [(k_{1,2}^{\text{Re}})^2 - (k_{1,2}^{\text{Im}})^2] = \varepsilon - E_{1,2}^{\text{th}} = \Delta_{1,2}. \quad (82)$$

Thus, by dividing both equations by $(k_{1,2}^{\text{Re}})^2$ and substituting one into the other, we get that

$$z_{1,2} = \frac{\lambda_{1,2} - \Delta_{1,2}}{\Gamma/2}, \quad (83)$$

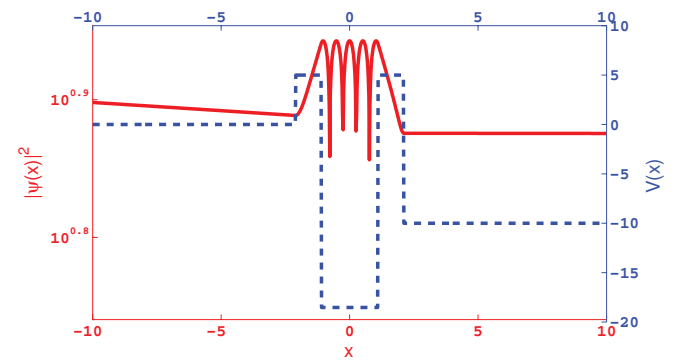


FIG. 5. (Color online) The constant piecewise potential (dashed blue line) and unscaled resonance wave function on a logarithmic scale (solid red line). All values are given in atomic units. The resonance energy is given by the position $\varepsilon = 1.45 \times 10^{-4}$ and the width $\Gamma = 6.13 \times 10^{-3}$.

TABLE III. Values of the partial widths and branching ratios in the old and new formulas for the constant piecewise potential in Fig. 5 (all values in atomic units).

	E_{res}	Method	Γ_-	Γ_+	$\Gamma_- + \Gamma_+$	$R = \frac{\Gamma_+}{\Gamma_-}$
ε	1.45×10^{-4}	MP	8.13×10^{-7}	1.88×10^{-5}	1.96×10^{-5}	23.12
Γ	6.13×10^{-3}	GGM	1.86×10^{-4}	5.94×10^{-3}	6.13×10^{-3}	31.94

where

$$\lambda_{1,2} = \sqrt{\Delta_{1,2}^2 + (\Gamma/2)^2}. \quad (84)$$

If we now substitute this into the expression for γ , we get that

$$\gamma = \frac{k_2^{\text{Re}}}{k_1^{\text{Re}}} \sqrt{\frac{\lambda_2(\lambda_2 - \Delta_2)}{\lambda_1(\lambda_1 - \Delta_1)}}. \quad (85)$$

This expression enables us to understand why there is no significant change when we use the new branching ratio over the old. To do so, we examine the geometrical relationship between the various terms in γ in Fig. 4.

When the two threshold are close with respect to the position of the resonance (i.e., $\Delta_{1,2} \ll \varepsilon$), then approximately $\Delta_1 \approx \Delta_2$ and $\lambda_1 \approx \lambda_2$; thus, no significant effect on γ is expected. We now examine the other extreme when one of the thresholds is very close to the resonance position but the other is far, that is, $\Delta_1 \ll \Delta_2$. In this case, again two extreme scenarios are possible: Either $\lambda_2 \gg \lambda_1$ when Γ is very small or when the Γ is much greater than both $\Delta_{1,2}$ then $\lambda_2 \approx \lambda_1 \approx \Gamma/2$. In the second scenario $\lambda_{1,2} - \Delta_{1,2} \approx \Gamma/2$ and once again no effect is expected on the branching ratio. Returning to the first option when $\lambda_2 \gg \lambda_1$, we can expect to see a significant effect on the branching ratio; however, as we increase the ratio λ_2/λ_1 by moving the second threshold further apart, it is clearly evident from Fig. 4 that in this case $\lambda_1 \approx \Gamma/2$ and thus $\lambda_2 - \Delta_2 \ll \lambda_1 - \Delta_1$. This means that we will have an opposing trend and thus again no major effect on the overall result. The only case where there might be an observable effect must lie somewhere between where the distance of the second threshold from the resonance will be comparable (i.e., within two orders of magnitude) to its width while still maintaining the first threshold close to the resonance position. We must always remember, though, that the “best” effect we will see will be just a factor of 1.41.

To find a resonance which satisfies the preceding conditions, we chose the constant piecewise potential depicted in Fig. 5 which can be solved analytically.

Manipulating the potential parameters we are able to move a long-living resonance between the barriers close enough to the top threshold to satisfy the preceding conditions. The partial widths and branching ratio for this resonance, which

are pictured in Fig. 5, are listed in Table III. We see that there is a significant difference between the two methods almost up to the maximum as $R_{\text{new}} = 1.38R_{\text{old}}$

VI. CONCLUDING REMARKS

By carrying out a rigorous asymptotic analysis of the tail of the resonance function, we obtained a unique expression for the partial widths which ensures that the sum of all the partial widths will add up to the total width. Our derivation was based on the TDSE but using a wave function with outgoing boundary condition. From this derivation it is evident that one can evaluate partial width and branching ratios based only on the parameters of the asymptote of the resonance wave function. The relevant parameters can be evaluated by any of the common methods used to obtain resonances. We showed that the only difference from the previously used MP formula for branching ratios and partial widths was in using the real part of the complex wave vector instead of the complex wave vector itself.

We have shown that, in general, one can hardly detect any difference in the branching ratios between the previous method and the one presented in this article and that the maximal possible difference is a factor of $\sqrt{2}$. In order for this difference to be significant, two conditions must hold:

- (i) the difference in energy between the two thresholds E_n and $E_{n'}$ must be large with respect to the distance of the resonance position to the upper threshold such that $\varepsilon - E_n^{\text{th}} \gg \varepsilon - E_{n'}^{\text{th}}$;
- (ii) the distance of the resonance position from the upper threshold should be comparable to the resonance width.

This difference will be evident when studying scattering problems of resonances near the threshold.

ACKNOWLEDGMENTS

We thank Kiyoshi Kato and Hiroshi Masui for raising the question of whether the partial widths obtained from complex scaling calculations sum up to the total width. The authors acknowledge the Minerva center for nonlinear physics of complex systems and the ISF (Grant No. 96/07) for their support.

- [1] G. Gamow, *Z. Phys.* **51**, 204 (1928); G. Gamow and C. L. Critchfield, *Theory of Atomic Nucleus and Nuclear Energy-Sources* (Clarendon, Oxford, 1949).
- [2] J. R. Taylor, *Scattering Theory: The Quantum Theory of Non-relativistic Collisions* (Wiley, New York, 1972).

- [3] D. Maruce, *Theory of Dielectric Optical Waveguides* (Academic Press, Boston, MA, 1991).
- [4] I. Vorobeichik, U. Peskin, and N. Moiseyev, *J. Opt. Soc. Am. B* **12**, 1133 (1995).
- [5] U. Peskin and N. Moiseyev, *J. Chem. Phys.* **96**, 2347 (1992).

- [6] R. Schinke, *Photodissociation Dynamics: Spectroscopy and Fragmentation of Small Polyatomic Molecules* (Cambridge University Press, Cambridge, 1993).
- [7] A. M. Perelomov and Ya. B. Zel'dovich, *Quantum Mechanics* (World Scientific, Singapore, 1998).
- [8] N. Moiseyev, *Phys. Rep.* **302**, 211 (1998).
- [9] O. I. Tolstikhin, V. N. Ostrovsky, and H. Nakamura, *Phys. Rev. A* **63**, 042707 (2001).
- [10] J. Okolowicz, M. Ploszajczak, and I. Rotter, *Phys. Rep.* **374**, 271 (2003).
- [11] F. C. Barker, *Phys. Rev. C* **68**, 054602 (2003).
- [12] V. N. Ostrovsky and N. Elander, *Chem. Phys. Lett.* **411**, 155 (2005).
- [13] N. Moiseyev and U. Peskin, *Phys. Rev. A* **42**, 255 (1990).
- [14] U. Peskin, N. Moiseyev, and R. Lefebvre, *J. Chem. Phys.* **92**, 2902 (1990).
- [15] M. Sakai, Y. Matsuda, M. Hirano, and K. Kato, *Few-Body Syst.* **46**, 189 (2009).
- [16] T. Noro and H. S. Taylor, *J. Phys. B* **13**, L377 (1980).
- [17] G. García-Calderón and A. Rubio, *Phys. Rev. B* **46**, 9784 (1992).
- [18] G. García-Calderón, R. Romo, and A. Rubio, *Phys. Rev. B* **47**, 9572 (1993).
- [19] N. Hatano, K. Sasada, H. Nakamura, and T. Petrosky, *Prog. Theor. Phys.* **119**, 187 (2008).
- [20] N. Moiseyev, P. R. Certain, and F. Weinhold, *Mol. Phys.* **36**, 1613 (1978).
- [21] H. Masui, S. Aoyama, T. Myo, and K. Kato, *Prog. Theor. Phys.* **102**, 1119 (1999).